Molecular Vision 2020; 26:742-756 <http://www.molvis.org/molvis/v26/742>
Received 28 April 2020 | Accepted 23 November 2020 | Published 25 November 2020

Role of *inhibitor of differentiation 3 gene* in cellular differentiation of human corneal stromal fibroblasts

Suneel Gupta,[1,2] Lynn M. Martin,[1,2] Nishant R. Sinha,[1,2] Kaitlin E. Smith,[1,3] Prashant R. Sinha,[1,2] Emilee M. Dailey,[1,3] Nathan P. Hesemann,[1,3] Rajiv R. Mohan[1,2,3]

[1]Harry S. Truman Memorial Veterans' Hospital, Columbia, MO; [2]One-Health Vision Research Program, Department of Veterinary Medicine & Surgery and Biomedical Sciences, College of Veterinary Medicine, University of Missouri, Columbia, MO; [3]Mason Eye Institute, School of Medicine, University of Missouri, Columbia, MO

Purpose: Inhibitor of differentiation (Id) proteins are helix–loop–helix (HLH) transcriptional repressors that modulate a range of developmental and cellular processes, including cell differentiation and cell cycle mobilization. The *inhibitor of differentiation 3 (Id3) gene*, a member of the *Id gene* family, governs the expression and progression of transforming growth factor beta (TGFβ)-mediated cell differentiation. In the face of mechanical, chemical, or surgical corneal insults, corneal keratocytes differentiate into myofibroblasts for wound repair. Excessive development or persistence or both of myofibroblasts after wound repair results in corneal haze that compromises corneal clarity and visual function. The objective of this study was to investigate whether Id3 overexpression in human corneal stromal fibroblasts governs TGFβ-driven cellular differentiation and inhibits keratocyte to myofibroblast transformation.

Methods: Primary human corneal stromal fibroblast (h-CSF) cultures were generated from donor human corneas. Human corneal myofibroblasts (h-CMFs) were produced by growing h-CSF in the presence of TGFβ1 under serum-free conditions. The *Id3 gene* was cloned into a mammalian expression vector (pcDNA3 mCherry LIC cloning vector), and the nucleotide sequence of the vector constructs was confirmed with sequencing as well as through restriction enzyme analysis. The *Id3* mammalian overexpression vector was introduced into h-CSFs using a lipofectamine transfection kit. The expression of Id3 in selected clones was characterized with quantitative real-time PCR (qRT–PCR), immunocytochemistry, and western blotting. Phase contrast microscopy and trypan blue exclusion assays were used to evaluate the effects of the transfer of the *Id3 gene* on the hCSF phenotype and viability, respectively. To analyze the inhibitory effects of the *Id3 gene* transfer on TGFβ-induced formation of h-CMFs, expression of the mRNA and protein of the myofibroblast marker alpha smooth muscle actin (α-SMA) was examined with qRT–PCR, western blotting, and immunocytochemistry. Student *t* test, analysis of variance (ANOVA), and Bonferroni adjustment for repeated measures were used for statistical analysis.

Results: The results indicate that Id3 overexpression does not alter the cellular phenotype or viability of h-CSFs. Overexpression of the *Id3 gene* in h-CSF cells grown in the presence of TGFβ1 under serum-free conditions showed a statistically significant decrease (76.3±4.3%) in α-SMA expression ($p<0.01$) compared to the naked-vector transfected or non-transfected h-CSF cells. Id3-transfected, naked-vector transfected, and non-transfected h-CSF cells grown in the absence of TGFβ1 showed the expected low expression of α-SMA (0–5%). Furthermore, *Id3* overexpression statistically significantly decreased TGFβ-induced mRNA levels of profibrogenic genes such as *fibronectin*, *collagen type I*, and *collagen type IV* (1.80±0.26-, 1.70±0.35- and 1.70±0.36-fold, respectively; $p<0.05$) that a play role in stromal matrix modulation and corneal wound healing. Results of the protein analysis with western blotting indicated that Id3 overexpression in h-CSF cells effectively slows TGFβ-driven differentiation and formation of h-CMFs. Results for subsequent overexpression studies showed that this process occurs through the regulation of E2A, a TATA box protein.

Conclusions: Id3 regulates TGFβ-driven differentiation of h-CSFs and formation of h-CMFs in vitro. Targeted *Id3 gene* delivery has potential to treat corneal fibrosis and reestablish corneal clarity in vivo.

The loss of corneal transparency and the development of scars (haze) after ocular insults are the leading cause of global blindness [1-3]. The molecular mechanisms and cell-signaling pathways that play a role in the initiation or progression of corneal haze, and approaches for preventing pathological wound repair and promoting scar-free repair have been extensively studied using various experimental models [2-8]. We, and others, have found that numerous growth factors and cytokines command origination of wound-repairing myofibroblasts and the development of haze during corneal wound healing [2-8]. Corneal stromal fibroblasts grown in the presence of transforming growth factor β (TGFβ) under serum-free conditions express significantly increased level of α-smooth muscle actin (α-SMA), a myofibroblast biomarker [3-7]. TGFβ is a multifunctional cytokine that regulates many

Correspondence to: Rajiv R. Mohan, Professor of Ophthalmology and Molecular Medicine, University of Missouri, 1600 E. Rollins St, Columbia, MO 65211; Phone+1-573-884-1449; FAX: +1-573-884-4100; email: mohanr@health.missouri.edu

cellular processes, including wound healing, angiogenesis, proliferation, differentiation, and apoptosis after traumatic insult by modulating different types of transcription factors, including the runt-related transcription factor 1 *(RUNX1*, Gene ID: 600349, OMIM 151385*)*, basic helix–loop–helix (*BHLHE41*, Gene ID: 600386, OMIM 606200), forkhead transcription factor (*FOXE1*, Gene ID: 600277, OMIM 602617), specificity protein 1 (*SP1*, Gene ID: 600581, OMIM 189906), activator protein 1 (*JUN*, OMIM 165160), and *inhibitor of differentiation* genes [9-12]. Furthermore, TGFβ influences more than 200 bHLH family members from yeast to humans [13]. The bHLH proteins play an essential role in directing cell fate by regulating the transcription of various genes [13-15]. A conserved bHLH domain, consisting of two amphipathic helixes that facilitate homo- or heterodimerization or both is a distinctive feature of this family [15]. Our previous studies exposed the association of transcriptional activity of bHLH proteins in TGFβ-driven fibrotic signaling in the cornea [16].

Inhibitor of differentiation proteins are DNA-binding transcription factors and have been implicated in the regulation of cell proliferation, migration, differentiation, inflammation, angiogenesis, and fibrosis [16-18]. Four *Id* genes (*Id1* to *Id4*) exist in mammals, and we previously characterized the existence and expression of all four *Id genes* in the cornea [16]. Members of the *Id gene* family have similar amino acid sequences within their HLH domain [18]. Researchers revealed that Id proteins act as transcriptional regulators in a dominant-negative manner by dimerizing with unique bHLH transcription factors [19]. The DNA binding activity of *Id genes* works as a functional inhibitor of bHLH transcription factors and regulates cell cycle progression. bHLH transcription factors control tissue-specific gene expression and regulate the transcription of target genes containing E-boxes in their promoters [20]. Id proteins show unique spatiotemporal arrangements during development and cell cycle progression, although evidence indicates biochemical redundancy in vitro [20]. The molecular mechanisms controlling Id protein expression are complex. Studies conducted during the last decade indicate that the transcription machinery of the *Id gene* is sensitive to stimulation from the extracellular environment, including cytokines like TGFβ, Smads, and BMP7 [2,5,21-23].

The *Id3* (OMIM 600277) gene was first reported in 1991 in mice (GenBank Accession # 3399) and located on chromosome 1. It consists of three coding exons and two introns [24]. The Id3 protein (15 kDa) is a member of the Id family of class V HLH proteins, which are 119 amino acids long [25]. Various in vivo studies on mice have shown that *Id3* plays a role in embryonic development through interaction with *Id1* and *Id2* [26,27]. In adult rodents, *Id3* is an early responsive gene with expression levels increasing in response to growth factor stimulation [28]. The Id3 protein, as implied by its name, was initially thought to be an inhibitor of cell differentiation [28,29]. Researchers contend that the loss or gain of Id protein function can lead to cellular makeover [20,30,31]. Id3 has been shown to be involved in the differentiation of many cell types, including fibroblasts, preadipocytes, and myofibroblasts [26-29]. However, recently the role of Id3 as a global differentiation blocker has been questioned [31-33].

In the cornea, our research indicates that the association between TGFβ hyperactivity and *Id genes* regulates the transcriptional machinery during corneal wound healing. This prompted us to postulate that the overexpression of the *Id3 gene* in corneal stromal fibroblasts impede excessive myofibroblast generation in stroma and subsequent haze formation in the cornea. In this study, we examined whether overexpression of the *Id3 gene* can control TGFβ1-mediated corneal fibroblast differentiation and investigated the underlying mechanism using an in vitro human corneal fibrosis model.

METHODS

Primary human corneal stromal fibroblast and myofibroblast cultures: An Institutional Review Board approved the study and the study adhered to the tenets of the Declaration of Helsinki and the ARVO statement on use of human donor tissues. Primary human corneal stromal fibroblasts (h-CSFs) were generated from donor human corneas obtained from an eye bank (Saving Sight, Kansas City, MO) using methods described previously [34]. Briefly, the epithelial and endothelial layers of the corneal tissues were removed with mild scraping with a scalpel blade, and residual corneal tissue was washed with Minimum Essential Medium (MEM; Gibco, Life Technology Corp., Grand Island, NY). The corneal tissue was divided into small pieces, placed in 100 × 20 mm cell culture dishes (Corning Inc., Corning, NY) with MEM supplemented with 10% fetal bovine serum (Thermo Fisher Scientific, Grand Island, NY), and incubated at 37 °C in 5% CO_2 for 3–5 weeks to obtain h-CSFs. h-CSF cells with 70% confluence were then used for experiments from two to five passages. Human corneal myofibroblast (h-CMF) cultures were produced by culturing h-CSFs in the presence of TGFβ1 (5 ng/ml; PeproTech Inc., Rocky Hill, NJ) under serum-free conditions, and cultures were incubated at 37 °C in 5% CO_2 for 72 h.

Vector generation, transfection, and selection of stable clones: To generate a mammalian expression vector-construct expressing the *Id3 gene*, PCR-amplified human *Id3 gene* (Accession number NM_002167) product (about 950 bp)

was cloned in pcDNA3 mCherry LIC mammalian expression vector using standard molecular biologic techniques [35]. Restriction mapping and DNA sequencing were used to confirm the nucleotide sequence of the pcDNA3 mCherry *Id3* vector construct and was termed *Id3*-transfected or *Id3*-mCherry for the entire study. Lipofectamine 3000 (Invitrogen, Life Technology Corp.) was used to deliver the *Id3*-mCherry plasmid into the h-CSF culture following the manufacturer's instructions. Briefly, 250 µl of DNA-lipid transfection solution was added dropwise to each well of the six-well plate by mixing equal volumes (125 µl) of Lipofectamine 3000 (7.5 µl) and plasmid DNA (5 µg DNA in 10 µl P3000) diluted with Opti-MEM and incubated for 15 min at room temperature. Cultures were then incubated at 37 °C in a humidified CO_2 incubator for 8 h, washed with Opti-MEM, and incubated for 72 h in MEM supplemented with 10% serum. The stably transfected clones overexpressing the *Id3 gene* were identified by subjecting the transfected cultures to gentamicin (G418 sulfate; 250–400 µg/ml) selection (Thermo Fisher) following the standard molecular biologic protocol.

Cellular morphology, viability, and growth profile: To monitor and record cellular morphology and the phenotypic progression at various time points for the cells, a Leica DMIL phase contrast microscope equipped with the Leica DFC290 imaging system (Leica Microsystems Inc., Buffalo Grove, IL) was used. Trypan blue exclusion dye and 3-(4,5-dimethylthiazol-2-yl)-2,5-diphenyltetrazolium bromide (MTT) assays using the CellTiter 96® Non-Radioactive Cell Proliferation Assay Kit (Thermo Fisher) were performed to determine the cellular viability, growth, and proliferation profile of the cells following published protocols [35]. Concisely, cells were trypsinized, and suspended in 0.4% trypan blue solution at various time points. Dead cells appeared blue as the dye entered the interior of the cells because of a broken membrane; live cells remained white due to intact membranes. Cell counts were performed with Neubauer's counting chamber (Thermo Fisher), and cellular viability was calculated and expressed in percentage of live cells in culture. Viability assays were performed to monitor the cellular growth profile of Id3-delivered and un-delivered cells.

Extraction of mRNA, cDNA synthesis, and quantitative real-time PCR: The RNeasy kit (Qiagen Inc., Valencia, CA) was used to extract mRNA from harvested cells and was reverse transcribed into cDNA using a commercial kit (Promega, Madison, WI) following the manufacturer's instructions. Quantitative real-time PCR (qRT–PCR) was performed using All-in-One qPCR mix (GeneCopoeia, Rockville, MD) in accordance with the manufacturer's instructions. Briefly, each 20 µl reaction contained 10 µl 2X All-in-One qPCR mix, 2 µl cDNA (0.5 µg), 2 µl forward primer (0.2 µM), and 2 µl reverse primer (0.2 µM), and 4 µl RNase and DNase free water and ran at a universal cycle (95 °C for 3 min, 40 cycles of 95 °C for 30 s followed by 60 °C for 60 s) following the published protocol [32]. The nucleotide sequences of the primers (forward and reverse) used for amplification in this study are provided in Table 1. Beta actin (β-actin) was used as a housekeeping gene to normalize the qRT–PCR data and verify the quality of the cDNA. The threshold cycle (Ct) was used to detect the increase in the signal associated with exponential growth of the PCR product during the log-linear phase. The relative mRNA expression was calculated using the following formula, $2\Delta\Delta Ct$. The ΔCt validation showed similar amplification efficiency for all templates used (the difference between linear slopes for all templates was less than 0.1).

Protein extraction and immunoblotting: To extract proteins, the cells were washed with ice-cold PBS (1X; pH 7.4; 137 mM NaCl, 2.7 mM KCl, 11.9 mM Phosphates) and lysed with a radioimmunoprecipitation assay (RIPA) buffer (50 mM Tris-HCl, pH 7.5, 150 mM NaCl, 1% NP-40, 0.5% sodium deoxycholate) containing a protease inhibitor mixture (Roche Applied Sciences, Indianapolis, IN). Debris and other residue were removed with centrifugation at 14,000 ×*g* at 4 °C, and clear protein lysate was collected for protein estimation using the Bio-Rad assay (Bio-Rad Life Sciences, Hercules, CA) [34].

Western blotting was performed using a standardized protocol [34]. Briefly, protein samples in Laemmli's sample buffer containing β-mercaptoethanol at 70 °C for 10 min were denatured. Proteins were resolved on 4–10% sodium dodecyl sulfate–polyacrylamide gel electrophoresis (SDS–PAGE) and transferred onto a 0.45 µm pore size polyvinylidene difluoride (PVDF) membrane using the Xcell-II blot module (Thermo Fisher). The membrane was blocked with 3% bovine serum albumin (BSA; Santa Cruz Biotechnology Inc., Dallas, TX) in Tris-buffered saline containing 0.1% Tween-20 detergent (TBST) for 1 h and probed with primary antibodies and housekeeping antibodies (1:100 dilution) in TBST followed by secondary anti-mouse or -goat antibodies (1:20,000 dilution). National Institutes of Health (NIH; (Bethesda, MD) ImageJ 1.38X image analysis software was used for digital quantification of detected protein bands using densitometry analysis.

Immunocytochemistry and fluorescence microscopy: Immunocytochemistry and fluorescence microscopy were performed to characterize and quantify α-SMA, a myofibroblast marker, to determine the levels of myofibroblasts and fibrosis using a mouse monoclonal antibody for α-SMA (Dako, Agilent Technologies, Carpinteria, CA). The

Table 1. Sequence of primers used in the study.

Gene Name	Forward Primer (5′ − 3′)	Reverse Primer (5′ − 3′)	Accesion No.	Species	Amplicon size (bp)
For Real Time PCR					
β-actin	CGGCTACAGCTTCACCACCA	CAGGCAGCTCGTAGCTCTTC	X_00351	Human	143
α-Smooth muscle actin	TGGGTGACGAAGCACAGAGC	CTTCAGGGGCAACACGAAGC	NM_001613	Human	138
Fibronectin	CGCAGCTTCGAGATCAGTGC	TCGACGGGATCACACTTCCA	NM_002026	Human	142
Collagen I	TGTGGCCCAGAAGAACTGGTACAT	ACTGGAATCCATCGGTCATGCTCT	NM_001845	Human	88
Collagen IV	AGGTGTTGACGGCTTACCTG	TTGAGTCCCGGTAGACCAAC	NM_000088.3	Human	132
For Regular PCR					
β-actin	AGGCCAACCGCGAGAAGATGACC	GAAGTCCAGGGCGACGTAGCAC	X_00351	Human	350
Id3-mCherry	CGCGTCATCGACTACATTCTC	CCCATGGTCTTCTTCTGCATT	NA	NA	617
Id3	ATTAAGCTTGCCACCATGAA GGCGCTGAGCCCGGTGCGCG	TCGGGATCCTGGCAAAAGCTCCT TTTGTCGTTGGAGATGAC	NM_002167	Human	390

Note: Sequence of the forward and reverse primers were used in the study to confirm the expression of different proteins on mRNA level using RT–PCR or to confirm the expression of protein through regular PCR amplification. bp=basepairs; NA=not applicable.

Id3-delivered, naked-vector delivered, and normal h-CSF cells were grown in the presence or absence of TGFβ1 (5 ng/ml) under serum-free conditions for 72 h, fixed with 4% freshly prepared paraformaldehyde. For immunostaining, fixed cells were washed twice with ice-cold PBS and blocked with 2% BSA (SC2323, Santa Cruz Biotechnology). Mouse monoclonal antibody for α-SMA was used at a 1:200 dilution in 1X PBS for 90 min followed by secondary antibody Alexa 488 or 594 goat anti-mouse IgG (Invitrogen, Molecular Probes, Life Technologies Corp., Eugene, OR) at a dilution of 1:500 for 1 h. Cells were mounted with Vectashield containing 4′,6-diamidino-2-phenylindole (DAPI; Vector Laboratories, Burlingame, CA) for visualization of the nuclei. Irrelevant isotype-matched primary antibody, secondary antibody alone, and tissue sections from naïve eyes were used as negative controls. Stained cells were visualized under a Leica fluorescence microscope (Leica, Wetzlar, Germany) and photographed with a digital camera (SpotCam RT KE, Diagnostic Instruments Inc., Sterling Heights, MI). The α-SMA-stained cells in ten randomly selected areas were counted per 200X and 400X magnification field.

Statistical analysis: Statistical analysis was performed using GraphPad Prism 6.07 software (GraphPad, La Jolla, CA). Statistical evaluation was executed using the Student *t* test and one-way ANOVA (ANOVA) followed by the Bonferroni multiple comparison test for post-hoc analysis in different cellular and molecular assays. The experiments were performed in triplicate (unless stated differently), and results of experiments are expressed with standard deviation (SD). Results of the experiment were considered statistically significant if the p value was less or equal to 0.05 from the total population.

RESULTS

Confirmation of delivered Id3 transcript: The quality of the cDNA and successful delivery of the plasmid-expressing *Id3 gene* in h-CSFs were confirmed with PCR amplification using primer sequences specific to the *β-actin gene* and the *Id3*-mCherry gene-insert cloned in the expression vector, respectively. Figure 1 shows an amplification product at 617 bp and confirmation of the presence of *Id3*-mCherry DNA in *Id3*-transfected cells. As expected, no amplification products (617 bp) were detected in the normal and naked-vector transfected cells. A band detected at 350 bp indicates the presence of β-actin, as the positive control. No amplification bands were detected in negative controls that had *Id3*-mCherry forward and reverse primers without cDNA.

Immunodetection of Id3-mCherry selected h-CSF clones: Cultures were subjected to immunocytochemistry to confirm the success of the gene transfer and expression of the *Id3-mCherry gene* inserted in the h-CSFs. Figure 2 shows representative images illustrating the expression of an mCherry fluorescent marker protein in h-CSF cells transfected with the *Id3*-mCherry plasmid (Figure 2H,I) and the absence of the fluorescent marker protein in normal (non-transfected) and naked-vector transfected cells (Figure 2A–F).

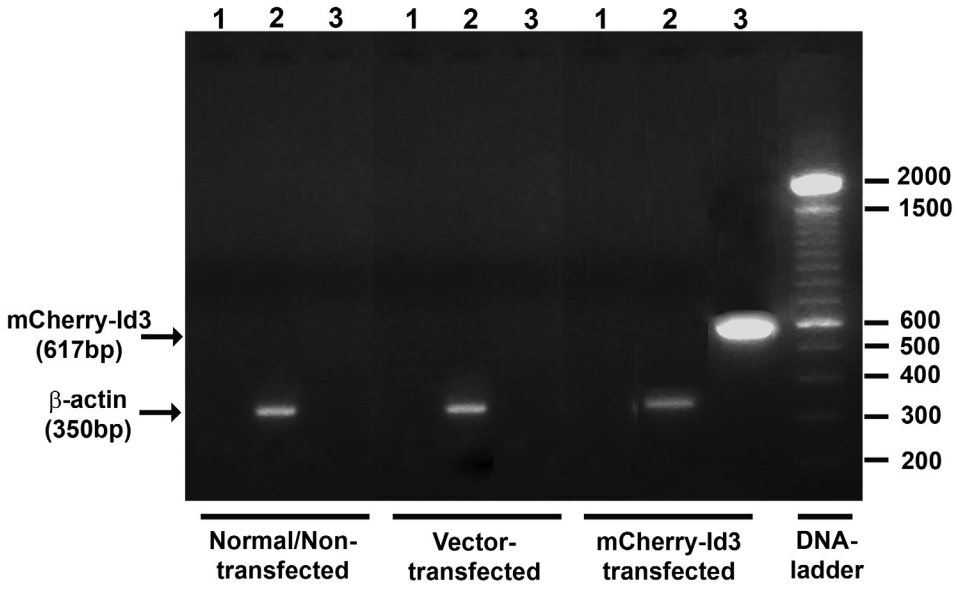

Figure 1. Agarose gel electrophoresis showing successful delivery of the *Id3-mCherry gene* into h-CSFs. An amplified *Id3-mCherry gene* product at 617 bp in *Id3*-mCherry human stromal corneal fibroblasts (h-CSFs; lane 3) was noted but not in the normal (lane 3) or naked-vector transfected (lane 3) h-CSFs. Negative controls containing *Id3*-mCherry forward and reverse primers without cDNA showed no amplification product (lane 1). The quality of the cDNA and PCR reagents was confirmed using β-actin forward and reverse primers (lane 2). The DNA ladder was 100 bp.

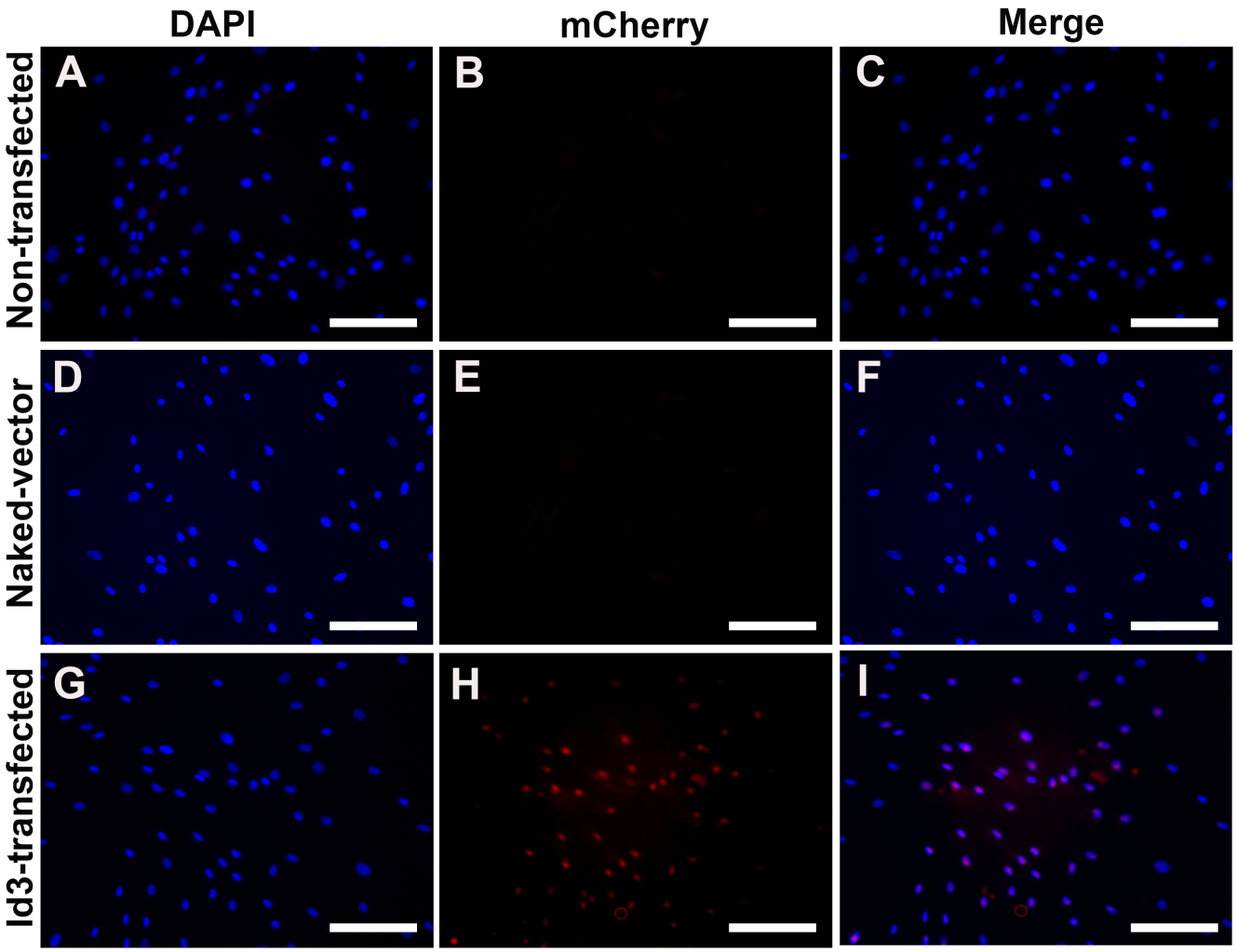

Figure 2. Immunofluorescence images showing the expression of the mCherry in human corneal fibroblast (h-CSFs) in normal and transfected cells. The *Id3*-mCherry transfected h-CSFs the successful transfection of *Id3* genes (**G-I**) but non-transfected (**A-C**) and naked-vector transfected (**D-F**) cells did not show Id3-mCherry expression as expected. Cells' nuclei were stained with DAPI (blue color) while *Id3*-mCherry protein were stained with mCherry (red color) respectively. Magnification bar: 100 µm.

Cellular morphology, viability, and growth profile: The cellular morphology of normal, naked-plasmid vector transfected, and *Id3*-mCherry transfected h-CSFs was examined under phase contrast microscopy. As evident from Figure 3, transfer of the *Id3 gene* did not alter the cellular morphology of the h-CSFs. Normal and transfected h-CSF cultures had spindle-shaped, flattened, and elongated morphology with contacts to neighboring cells, which is typical of corneal stromal fibroblasts when grown in MEM supplemented with 10% fetal bovine serum. The lack of differences in the cellular morphology between the *Id3*-mCherry-delivered cells (Figure 3C) and the normal (Figure 3A) or naked-vector delivered (Figure 3B) cells suggests that overexpression of *Id3* is nontoxic to h-CSFs.

Next, we determined the effects of overexpression of Id3 on h-CSF growth, proliferation, and viability using commercial assays. Figure 4 shows growth and proliferation profiles (Figure 4A), and cellular viabilities (Figure 4B) of normal, naked-vector delivered, and *Id3*-delivered h-CSFs. Screened *Id3*-delivered and naked-vector delivered h-CSFs showed growth patterns (Figure 4A), and cellular viability (Figure 4B) similar to those of the non-transfected or normal h-CSFs. As evident from the MTT data presented in Figure 4A, a non-statistically significant difference (4–8%; $p>0.05$) in the growth rate was observed among non-transfected or normal, naked-vector delivered, and Id3-delivered h-CSFs up to five tested passages. Furthermore, 94–98% cells were

found viable in three cell types in the trypan-blue assay and up to five tested passages as evident in Figure 4B.

Id3 regulates TGFβ1-driven cellular differentiation and myofibroblast production: To study the effect of the *Id3 gene* on TGFβ1-stimulated cell differentiation and myofibroblast generation, cultures were grown in the presence or absence of TGFβ1 (5 ng/ml) under serum-free conditions and analyzed for changes in cellular morphology and myofibroblast biomarker α-SMA protein levels. The phase contrast images in Figure 5 show the extent of cellular differentiation in normal non-transfected, naked-vector transfected, and *Id3*-transfected h-CSF cultures. As expected, TGFβ1 treatment in normal h-CSFs (Figure 5D) and naked-vector transfected h-CSFs (Figure 5E) induced transdifferentiation and produced phenotypic characteristics of the myofibroblasts. Conversely, *Id3*-overexpressing h-CSFs under similar conditions resisted cellular differentiation and maintained typical fibroblastic morphological characteristics (Figure 5F). None of these cells grown in the absence of TGFβ1 underwent cellular differentiation and acquired the myofibroblast phenotype (Figure 5A–C). This phenomenon was further verified with immunofluorescence using an antibody specific for the α-SMA protein.

Figure 6 shows the levels of the α-SMA protein in the *Id3*-transfected and normal non-transfected h-CSFs grown in the presence or absence of TGFβ1 under serum-free conditions. As evident from the panels, the *Id3*-transfected h-CSFs show statistically significantly decreased α-SMA immunostaining (Figure 6D) compared to the normal non-transfected h-CSFs grown in the presence of TGFβ1 (Figure 6C), but neither the *Id3*-transfected h-CSFs nor the normal non-transfected h-CSFs show any detectable α-SMA levels when grown in the absence of TGFβ1 (Figure 6A,B). This suggests that the *Id3 gene* negatively regulates cellular differentiation and myofibroblast production. The α-SMA protein levels of the naked-vector controls were found to be analogous in normal or non-transfected h-CSFs (data not shown). Figure 7 shows quantification of TGFβ1-induced h-CSF differentiation to myofibroblasts by the *Id3 gene*, which was statistically significant (76.3±4.30%; p<0.001).

Id3 governs profibrotic gene response in h-CSFs: The impact of the *Id3 gene* during fibrosis was analyzed by measuring the relative change in mRNA expression of profibrotic genes in cells induced by TGFβ1 that underwent cell differentiation and myofibroblast production. The *Id3*-transfected and normal non-transfected h-CSFs were grown in the presence or absence of TGFβ1 under serum-free media and mRNA levels of four fibrotic genes in the extracellular matrix (ECM) and were quantified with qRT–PCR. Figure 8 shows the relative change in the mRNA expression of the ECM genes, namely, α-*SMA*, *fibronectin*, and *collagen types I* and *IV*. TGFβ1 stimulation caused statistically significant increases in the expression of profibrogenic genes α-*SMA* (5.50±0.53-fold; p<0.001), *fibronectin* (3.10±0.26-fold; p<0.01), *collagen type I* (2.70±0.35-fold; p<0.01), and *collagen type IV* (2.20±0.36-fold; p<0.01) in normal, non-transfected h-CSFs. *Id3*-delivered h-CSFs significantly defied the TGFβ1-driven differentiation process, including the production of ECM components and profibrotic genes. *Id3*-transfected h-CSFs showed a statistically significant decrease in the mRNA levels of α-*SMA* (3.20±0.19-fold; p<0.001), *fibronectin* (1.80±0.26-fold; p<0.01), *collagen type I* (1.70±0.35-fold; p<0.01), and *collagen type IV* (1.70±0.36-fold; p<0.01) compared to those of normal, non-transfected h-CSFs under similar culture

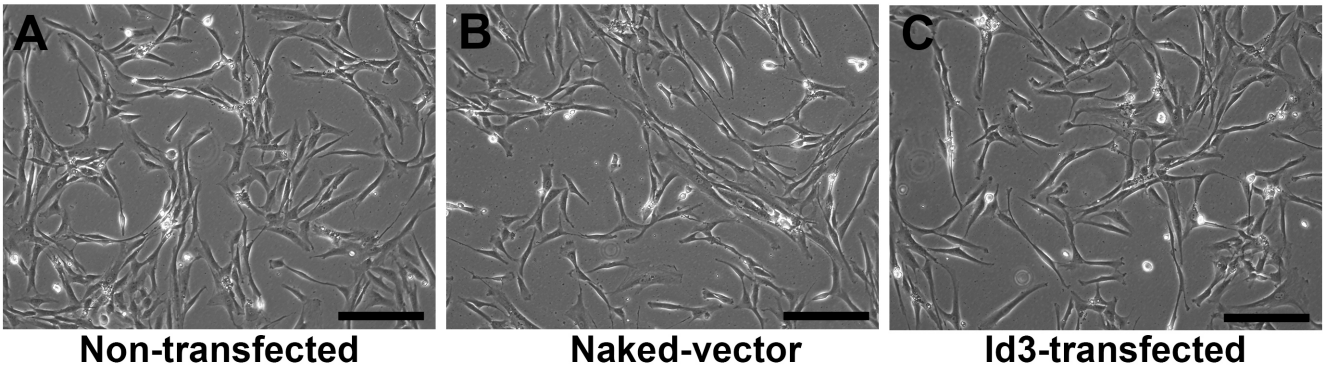

Figure 3. Representative phase contrast microscopy images revealing the phenotype of h-CSFs with and without gene transfer. **A**: Normal or non-transfected human stromal corneal fibroblasts (h-CSFs). **B**: Naked-vector transfected h-CSFs. **C**: *Id3*-mCherry transfected h-CSFs. No statistically significant differences in cellular phenotype were observed between the *Id3*-mCherry transfected h-CSFs (**C**) and the control groups (**A**, **B**). Magnification bar: 100 µm.

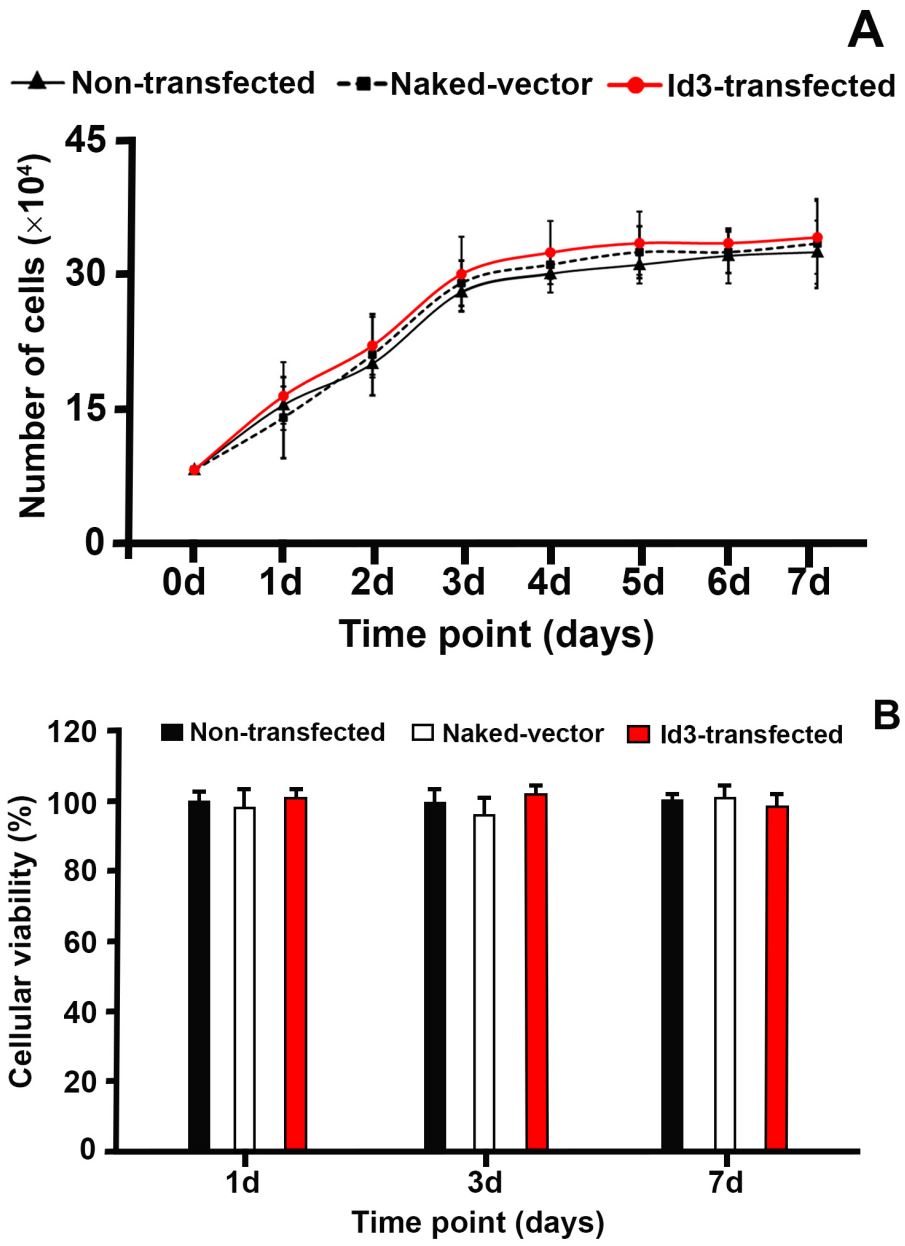

Figure 4. Proliferation and cellular viability of h-CSFs with or without gene transfer. **A**: Time-dependent growth profile of normal, naked-vector transfected, and *Id3*-mCherry transfected human stromal corneal fibroblast (h-CSF) cultures. **B**: Time-dependent cellular viability of normal, naked-vector transfected, and *Id3*-mCherry transfected h-CSF cultures. No statistically significant differences in the proliferation rate or cellular viability were observed between the *Id3*-mCherry transfected h-CSFs and the control groups (normal and naked-vector transfected h-CSFs).

conditions (Figure 8). The mRNA levels of these genes in naked-vector transfected h-CSFs were found to be analogous to those of normal non-transfected h-CSFs.

Id3 interacts with E-box protein and regulates cell differentiation: To characterize the molecular mechanism of the *Id3 gene* on the cellular differentiation event, we investigated the interactions of Id3 with the bHLH region of the E2A protein. Normal, non-transfected and *Id3*-transfected h-CSFs were grown in the presence or absence of TGFβ1, and the levels of the α-SMA and E2A proteins were quantified with western blotting. Figure 9 shows the results of western blotting and quantification of the Id3, α-SMA, and E2A proteins under normal and TGFβ1 influence. The increased α-SMA and Id3 protein levels with the associated decrease in the E2A protein level in the *Id3*-transfected h-CSFs compared to normal non-transfected h-CSFs grown under the influence of TGFβ1 (Figure 9A) suggest that negative regulation of cellular differentiation occurs via interactions of Id3 with the bHLH region of the E2A protein. This notion was further supported by the observation that no noticeable changes were detected in

the α-SMA and E2A protein levels, when these h-CSFs were grown in the absence of TGFβ1. The densitometry analysis of the western blotting data showed the decrease in the α-SMA (51.4±2.10%; p<0.001) and E2A protein levels (46.1±3.40%; p<0.001) in the *Id3*-transfected h-CSFs was statistically significant compared to that of the normal non-transfected h-CSFs (Figure 9B).

Molecular mechanism of Id3 overexpression govern differentiation cascades: The overexpression of Id3 attenuates TGFβ1/Smad-driven cell differentiation through a dominant negative effect by the DNA binding of the E-protein bHLH region. In the present study, we showed direct biochemical evidence of HLH proteins, Id3 and E2A with fibrosis marker α-SMA. We proposed the molecular mechanism that the formation of hetero-oligomeric complexes of Id3 with the E-protein of bHLH would modulate the differentiation cascade in h-CSFs (Figure 10).

DISCUSSION

TGFβ is a member of a superfamily of polypeptides that regulates cell cycle progression, differentiation, and chemotaxis of many different types of cells [2,5]. TGFβ also regulates a diverse set of essential cellular processes during the development of corneal fibrosis [3-7]. In response to corneal insults, endogenous epithelial-derived TGFβ drives populations of keratocytes to transdifferentiate into myofibroblasts, initiating the process of corneal wound healing. The developed myofibroblast cells undergo cellular matrix remodeling and result in ECM disorganization with abundant collagen type III and IV populations that contribute to loss of corneal transparency. Differentiation events include the production of ECM proteins, mediation of cell adhesion, and modulation of collagen fibrillogenesis governed through TGFβ/Smad signaling [5]. Ultimately, this leads to the development of corneal fibrosis. The information garnered from this study shows that overexpression of the *Id3 gene* inhibits TGFβ-modulated expression of profibrogenic genes and formation of myofibroblasts in h-CSFs.

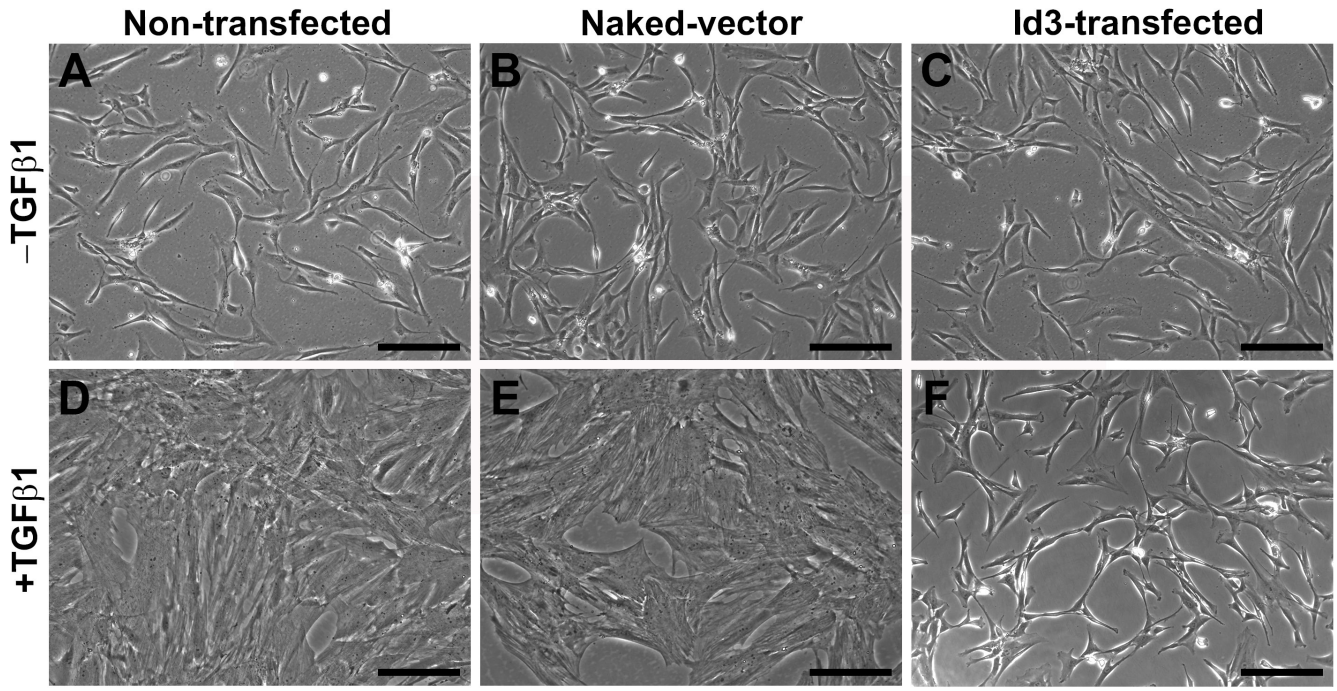

Figure 5. Phase contrast microscopy showing changes in the cellular phenotype of the h-CSFs grown in the presence or absence of TGFβ1 (5 ng/ml) in serum-free conditions with or without *Id3 gene* transfer. **A**: Normal human stromal corneal fibroblasts (h-CSFs) grown in the absence of transforming growth factor beta (TGFβ). **B**: Naked-vector transfected h-CSFs grown in the absence of TGFβ1. **C**: *Id3*-transfected h-CSFs grown in the absence of TGFβ1. **D**: Normal h-CSFs grown in the presence of TGFβ1. **E**: Naked-vector transfected h-CSFs grown in the presence of TGFβ1. **F**: *Id3*-transfected h-CSFs grown in the presence of TGFβ1. Overexpression of the *Id3 gene* in h-CSFs prevented TGFβ-induced cellular differentiation and change to the myofibroblast phenotype (**F**). Magnification bar: 50 µm.

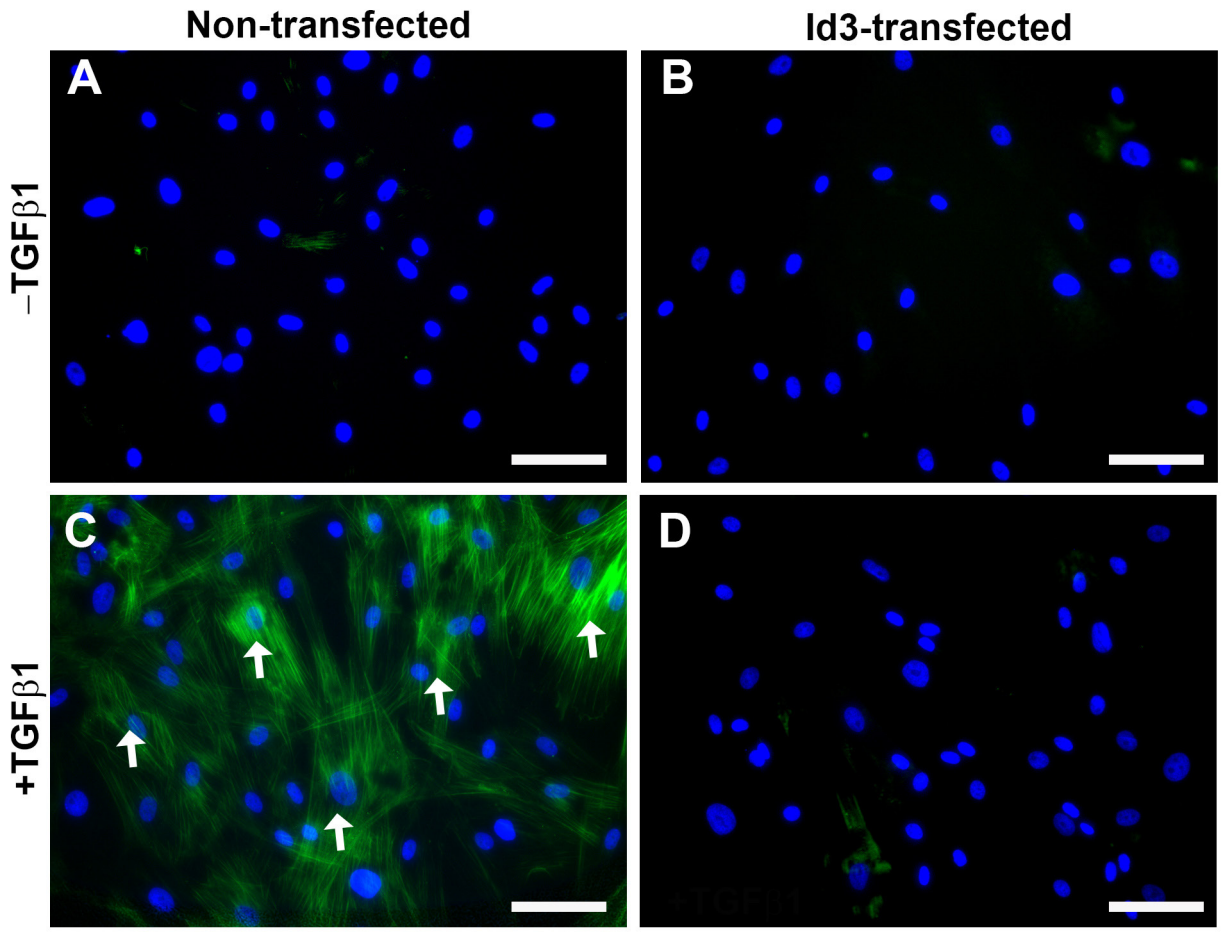

Figure 6. Representative immunofluorescence staining images reveal levels of α-SMA, a myofibroblast marker, and DAPI in h-CSFs. Cultures with or without *Id3 gene* transfer were grown in the absence or absence of transforming growth factor beta (TGFβ; 5 ng/ml) for 72 h under serum-free conditions. **A**: Normal human stromal corneal fibroblasts (h-CSFs) grown in the absence of TGFβ1. **B**: *Id3*-delivered h-CSFs grown in the absence of TGFβ1. **C**: Normal h-CSFs grown in the presence of TGFβ1. **D**: *Id3*-delivered h-CSFs grown in the presence of TGFβ1. TGFβ1 treatments caused a noticeable increase in α-SMA (green) in normal h-CSFs (**C**), but this response was prevented by overexpression of the *Id3 gene* in the h-CSFs (**D**). Non-TGFβ1-treated cultures mainly exhibited 4′,6-diamidino-2-phenylindole (DAPI) stained nuclei (blue) and the expected α-SMA staining in a few cells (**A** and **B**). Magnification bar: 50 µm.

Although several imminent novel TGFβ-responsive genes encoding transcription factors have been identified, in this study, we focused on the Id family of transcription factors, specifically Id3. Initial investigations of Id proteins focused on their role in development [27,36], and subsequent studies exposed a role for Id proteins in influencing many essential cellular functions, including cell proliferation, differentiation, survival, and invasion, along with angiogenesis, senescence, apoptosis, and metastasis [16-22]. Within Id proteins, the basic region of the bHLH protein is not present, and therefore, it cannot bind to the DNA directly. Id proteins have a dominant-negative effect by binding DNA bHLH proteins that drive cell lineage, commitment, and differentiation [37,38]. We previously reported the expression and role of Id1 to Id4 in human and rabbit normal and fibrotic corneas [16].

One trigger of the corneal fibrosis cascade is induction of reactive oxygen species (ROS) [19]. Current literature shows that Id3 regulates the differentiation phenomenon through induction of ROS in vascular epithelial cells due to redox-sensitive properties [19,38-40]. The results of the present study demonstrate that overexpression of the *Id3 gene* in h-CSFs attenuates the impact of profibrotic cytokines and modulates cellular differentiation, as well as wound healing cascades. These results are well supported by previous studies performed in myocytes that showed overexpression of Id proteins delayed the onset of differentiation [41]. The present study also revealed the underlying mechanism that the HLH

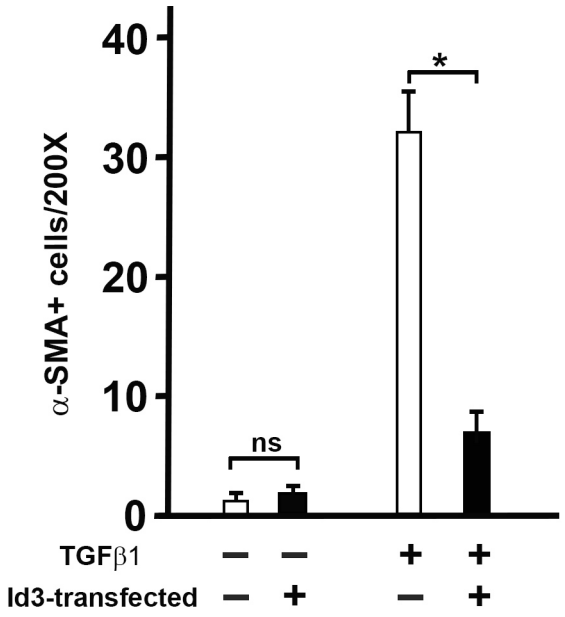

Figure 7. Quantification of α-SMA immunostaining. Data are mean ± standard deviation (SD, n = 3). *Significant attenuation of transforming growth factor beta (TGFβ)-induced alpha smooth muscle actin (α-SMA) was observed in human stromal corneal fibroblasts (h-CSFs) transfected with the *Id3 gene* (p<0.001).

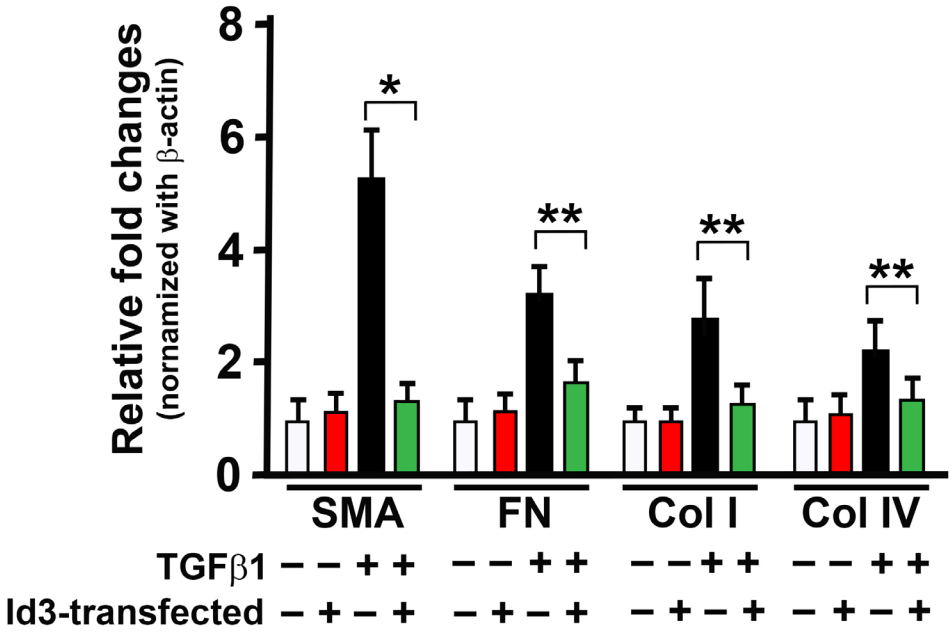

Figure 8. Quantitative RT–PCR showing effects of overexpression of the *Id3 gene* on the mRNA expression of profibrotic genes in the presence and absence of TGFβ1 (5 ng/ml). Data are mean ± standard deviation (SD, n = 3). Overexpression of the *Id3 gene* in human stromal corneal fibroblasts (h-CSFs) attenuated transforming growth factor beta (TGFβ)-induced the expression of the α-*SMA*, *fibronectin*, *collagen I*, and *collagen IV* genes statistically significantly (*p<0.001 and **p<0.01), but there was no change in these genes in the absence of TGFβ1.

proteins, Id3, and E2A can form hetero-oligomeric complexes that modulate the differentiation cascade. These findings corroborate many literature reports that showed Id proteins have the ability to act as an inhibitor of myofibroblast formation by associating with bHLH class A and E proteins (E12, E47, E2–2, and HEB) [41-45]. Conversely, other non-ocular studies reported the induction of Id3 expression by TGFβ, and this information suggests a role for Id3 in regulating the transcriptional responses of fibroblasts [21,43]. In this study, the mRNA and protein results indicate that Id3 overexpression controls TGFβ-mediated profibrotic events. The noticeable reduction in the mRNA expression of *collagens*

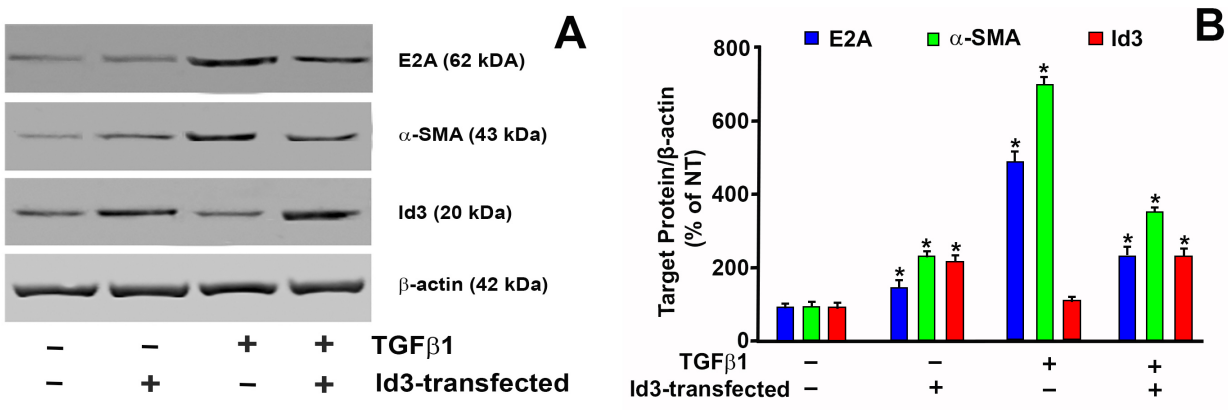

Figure 9. Immunoblotting of E2A, α-SMA, and Id3 showing interaction with bHLH E-protein in TGFβ1-induced cellular differentiation in h-CSFs. **A**: Representative immunoblots for E2A, alpha smooth muscle actin (α-SMA), Id3, and β-actin. **B**: Quantification of the corresponding densitometry data of the protein immunoblots. The protein expression was normalized to β-actin and represented as percentage change (%) compared to the no treatment control (in no transforming growth factor beta (TGFβ) and *Id3 gene* transfer groups). Data are mean ± standard deviation (SD, n = 3). *Significant difference from the no treatment control. This suggests that Id helix–loop–helix (HLH) proteins play a role in the cellular differentiation of human stromal corneal fibroblasts (h-CSFs) involving TGFβ1.

I and *IV* in *Id3*-overexpressing cells suggests that Id3 plays an important role in corneal matrix organization and TGFβ-induced differentiation. Results of this study reflect that *Id3* suppresses myofibroblast differentiation by controlling the bHLH protein. These findings correspond with preadipocyte literature and validate that Id3 either interacts directly with the bHLH protein or prevents the interaction of E2A proteins [29]. Ids heterodimerize through HLH motifs, which are highly conserved within this protein family. It is conceivable that all other isoforms of Ids interact with the same protein-binding site to regulate the differentiation process. Constitutive expression of Id3 also stops differentiation in adipose cells, but the effect of other Id proteins (Id1, Id2, and Id4) on differentiation has not been examined [29]. The protein data suggest a mechanistic role for Id3 and E-box proteins in the corneal fibroblast differentiation process; however, the data did not categorically establish a cause-and-effect relationship between the Id3 and E-box proteins. Our ongoing in vitro and in vivo studies characterizing mechanistic and functional roles of Id3 and E-box proteins on cellular differentiation of corneal fibroblasts will address this limitation, and fill gaps in knowledge. Furthermore, they are expected to exhibit whether suppression of TGFβ/Smad signaling by bHLH proteins through overexpression of the *Id3 gene* into corneal

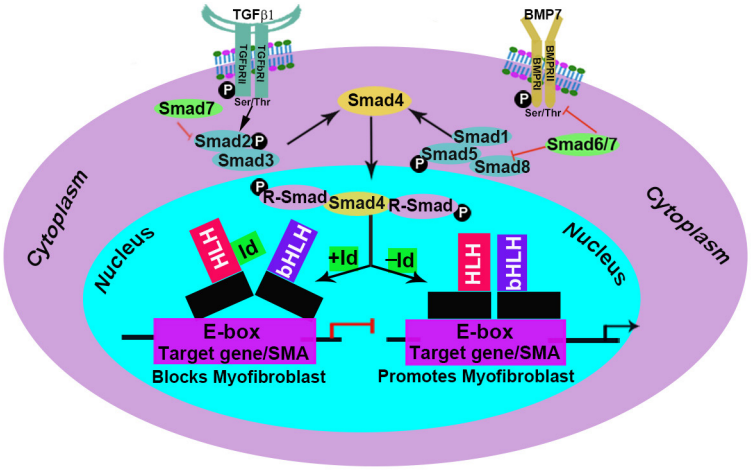

Figure 10. Schematic illustration showing inhibition of TGFβ1-induced cellular differentiation by *Id3 gene* transfer in h-CSFs.

stroma can offer clinically valuable modality to treat corneal opacity and restore corneal transparency in vivo.

Gene therapy in the cornea is a promising therapy for the prevention and treatment of visual disability due to corneal scarring [35]. Additionally, gene therapy to treat corneal scarring has been successfully demonstrated by delivering genes with an adenosine-associated viral or nanoparticle vector into rabbit and human keratocytes [7,8,25]. The potential of *Id3 gene* therapy to inhibit TGFβ-driven fibrosis has been reported in many non-ocular tissues employing various in vivo and in vitro models [21,29,32,33,44]. Our ongoing in vivo rabbit studies focus on developing gene therapies that reduce corneal scar or haze through the use of gain-of-function of Id3 overexpression by ectopic overexpression into corneal stroma to modulate the TGFβ/Smad signaling pathways.

In summary, overexpression of the *Id3 gene* downregulated profibrotic gene expression and effectively prevented TGFβ-driven transformation of h-CSFs into h-CMFs through the interaction of *Id3* with the basic region of the TATA box E-box protein. Based on these results, *Id3 gene* therapy warrants further investigation as a conceivable treatment for corneal fibrosis in vivo.

ACKNOWLEDGMENTS

This work was primarily supported by the 1I01BX000357, Veteran's Health Affairs Merit and Research Career Scientist grants (RRM), Washington DC, USA; and partially by the NIH/NEI 5R01EY017294; 5R01EY030774, and 1U01EY031650 grants (RRM) Bethesda, Maryland, USA, and the Ruth Kraeuchi Missouri Endowed Chair Ophthalmology Fund (RRM) University of Missouri, Columbia, Missouri, USA.

REFERENCES

1. Foster A, Resnikoff S. The impact of Vision 2020 on global blindness. Eye (Lond) 2005; 19:1133-5. [PMID: 16304595].
2. Saika S, Yamanaka O, Okada Y, Tanaka S, Miyamoto T, Sumioka T, Kitano A, Shirai K, Ikeda K. TGF beta in fibroproliferative diseases in the eye. Front Biosci 2009; 1:376-90. [PMID: 19482708].
3. Ljubimov AV, Saghizadeh M. Progress in corneal wound healing. Prog Retin Eye Res 2015; 49:17-45. [PMID: 26197361].
4. de Oliveira RC, Wilson SE. Fibrocytes, wound healing, and corneal fibrosis. Invest Ophthalmol Vis Sci 2020; 61:28-[PMID: 32084275].
5. Saika S, Yamanaka O, Okada Y, Sumioka T. Modulation of Smad signaling by non-TGFβ components in myofibroblast generation during wound healing in corneal stroma. Exp Eye Res 2016; 142:40-8. [PMID: 26675402].
6. Jester JV, Huang J, Petroll WM, Cavanagh HD. TGFbeta induced myofibroblast differentiation of rabbit keratocytes requires synergistic TGFbeta, PDGF and integrin signaling. Exp Eye Res 2002; 75:645-57. [PMID: 12470966].
7. Gupta S, Fink MK, Ghosh A, Tripathi R, Sinha PR, Sharma A, Hesemann NP, Chaurasia SS, Giuliano EA, Mohan RR. Novel Combination BMP7 and HGF gene therapy instigates selective myofibroblast apoptosis and reduces corneal haze *in vivo*. Invest Ophthalmol Vis Sci 2018; 59:1045-57. [PMID: 29490341].
8. Gupta S, Rodier JT, Sharma A, Giuliano EA, Sinha PR, Hesemann NP, Ghosh A, Mohan RR. Targeted AAV5-Smad7 gene therapy inhibits corneal scarring *in vivo* PLoS One 2017; 12:1-18. [PMID: 28339457].
9. Tzavlaki K, Moustakas A. TGF- beta signaling. Biomolecules 2020; 10:487-[PMID: 32210029].
10. Derynck R, Budi EH. Specificity, versatility, and control of TGF-β family signaling. Sci Signal 2019; 12:570-[PMID: 30808818].
11. Ito Y, Miyazono K. RUNX transcription factors as key targets of TGF-beta superfamily signaling. Curr Opin Genet Dev 2003; 13:43-7. [PMID: 12573434].
12. Meng X, Nikolic-Paterson D, Lan H. TGF-β: the master regulator of fibrosis. Nat Rev Nephrol 2016; 12:325-38. [PMID: 27108839].
13. Asirvatham AJ, Schmidt MA, Chaudhary J. Non-redundant inhibitor of differentiation (Id) gene expression and function in human prostate epithelial cells. Prostate 2006; 66:921-35. [PMID: 16541417].
14. Murre C. Helix-loop-helix proteins and the advent of cellular diversity: 30 years of discovery. Genes Dev 2019; 33:6-25. [PMID: 30602438].
15. Tarczewska A, Greb-Markiewicz B. The Significance of the Intrinsically Disordered Regions for the Functions of the bHLH Transcription Factors. Int J Mol Sci 2019; 20:5306-[PMID: 31653121].
16. Mohan RR, Morgan BR, Anumanthan G, Sharma A, Chaurasia SS, Rieger FG. Characterization of Inhibitor of differentiation (Id) proteins in human cornea. Exp Eye Res 2016; 146:145-53. [PMID: 26712606].
17. Roschger C, Cabrele C. The Id-protein family in developmental and cancer-associated pathways. Cell Commun Signal 2017; 15:7-[PMID: 28122577].
18. Ling F, Kang B, Sun XH. Chapter Five: Id Proteins. Small Molecules, mighty regulators. Curr Top Dev Biol 2014; 110:189-216. [PMID: 25248477].
19. Avecilla A, Doke M, Jovellanos J, Avecilla V. Contribution of inhibitor of differentiation and estrogenic endocrine disruptors to neurocognitive disorders. Med Sci. (Basel, Switzerland). 2018; 6(3).

20. Nair R, Teo WS, Mittal V, Swarbrick A. Reviews: ID proteins regulate diverse aspects of cancer progression and provide novel therapeutic opportunities. Mol Ther 2014; 22:1407-15. [PMID: 24827908].

21. Strong N, Millena AC, Walker L, Chaudhary J, Khan SA. Inhibitor of differentiation 1 (Id1) and Id3 proteins play different roles in TGFβ effects on cell proliferation and migration in prostate cancer cells. Prostate 2013; 73:624-33. [PMID: 23060149].

22. Chen DF, Cao J, Liu Y, Wu Y, Du SH, Li H, Zhou JH, Li YW, Zeng HP, Hua ZC. BMP-Id pathway targeted by cholesterol myristate suppresses the apoptosis of PC12 cells. Brain Res 2011; 1367:33-42. [PMID: 20970407].

23. Saika S, Ikeda K, Yamanaka O, Flanders KC, Ohnishi Y, Nakajima Y, Muragaki Y, Ooshima A. Adenoviral gene transfer of BMP-7, Id2, or Id3 suppresses injury-induced epithelial-to-mesenchymal transition of lens epithelium in mice. Am J Physiol Cell Physiol 2006; 290:C282-9. [PMID: 16120655].

24. Christy BA, Sanders LK, Lau LF, Copeland NG, Jenkins NA, Nathans D. An Id-related helix-loop-helix protein encoded by a growth factor-inducible gene. Proc Natl Acad Sci USA 1991; 88:1815-[PMID: 2000388].

25. Svendstrup M, Vestergaard H. Mini review: The potential role of inhibitor of differentiation-3 in human adipose tissue remodeling and metabolic health. Mol Genet Metab 2014; 113:149-54. [PMID: 25239768].

26. Atherton GT, Travers H, Deed R, Norton JD. Regulation of cell differentiation in C2C12 myoblasts by the Id3 helix-loop-helix protein. Cell Growth Differ 1996; 7:1059-66. [PMID: 8853902].

27. Jen Y, Manova K, Benezra R. Each member of the Id gene family exhibits a unique expression pattern in mouse gastrulation and neurogenesis. Dev Dyn 1997; 208:92-106. [PMID: 8989524].

28. Barone MV, Pepperkok R, Peverali FA, Philipson L. Id proteins control growth induction in mammalian cells. Proc Natl Acad Sci USA 1994; 91:4985-[PMID: 8197168].

29. Moldes M, Lasnier F, Fève B, Pairault J, Djian P. Id3 prevents differentiation of preadipose cells. Mol Cell Biol 1997; 17:1796-[PMID: 9121427].

30. Johnson AL, Haugen MJ, Woods DC. Role for inhibitor of differentiation/ deoxyribonucleic acid-binding (Id) proteins in granulosa cell differentiation. Endocrinology 2008; 149:3187-95. [PMID: 18325989].

31. Kondo M, Cubillo E, Tobiume K, Shirakihara T, Fukuda N, Suzuki H, Shimizu K. Takehara k, Cano A, Saitoh M, Miyazono K. A role for Id in the regulation of TGF-beta-induced epithelial-mesenchymal transdifferentiation. Cell Death Differ 2004; 11:1092-101. [PMID: 15181457].

32. Cutchins A, Harmon DB, Kirby JL, Doran AC, Oldham SN, Skaflen M, Klibanov AL, Meller N, Keller SR, Garmey J, McNamara CA. Inhibitor of differentiation-3 mediates high fat diet-induced visceral fat expansion. Arterioscler Thromb Vasc Biol 2012; 32:317-24. [PMID: 22075252].

33. Doran AC, Meller N, Cutchins A, Deliri H, Slayton RP, Oldham SN, Kim JB, Keller SR, McNamara CA. The Helix–Loop–Helix Factors Id3 and E47 Are Novel Regulators of Adiponectin. Circ Res 2008; 103:624-34. [PMID: 18669923].

34. Sharma A, Sinha NR, Siddiqui S, Mohan RR. Role of 5′TG3′-interacting factors (TGIFs) in vorinostat (HDAC inhibitor)-mediated corneal fibrosis inhibition. Mol Vis 2015; 21:974-84. [PMID: 26330748].

35. Mohan RR, Gupta R, Mehan MK, Cowden JW, Sinha S. Decorin transfection suppresses profibrogenic genes and myofibroblast formation in human corneal fibroblasts. Exp Eye Res 2010; 91:238-45. [PMID: 20546727].

36. Roschger C, Cabrele C. The Id-protein family in developmental and cancer-associated pathways. Cell Commun Signal 2017; 15:7-[PMID: 28122577].

37. Chambers RC, Leoni P, Kaminski N, Laurent GJ, Heller RA. Global expression profiling of fibroblast responses to transforming growth factor-β1 reveals the induction of inhibitor of differentiation-1 and provides evidence of smooth muscle cell phenotypic switching. Am J Pathol 2003; 162:533-46. [PMID: 12547711].

38. Bensellam M, Montgomery MK, Luzuriaga J, Chan JY, Laybutt DR. Inhibitor of differentiation proteins protect against oxidative stress by regulating the antioxidant-mitochondrial response in mouse beta cells. Diabetologia 2015; 58:758-70. [PMID: 25636209].

39. Lee YS, Yoon S, Yoon HJ, Lee K, Yoon HK, Lee JH. Song CWl. Inhibitor of differentiation 1 (Id1) expression attenuates the degree of TiO2-induced cytotoxicity in H1299 non-small cell lung cancer cells. Toxicol Lett 2009; 189:191-9. [PMID: 19486931].

40. Lin J, Guan Z, Wang C, Feng L, Zheng Y, Caicedo E, Bearth E, Peng JR, Gaffney P, Ondrey FG. Inhibitor of Differentiation 1 Contributes to head and neck squamous cell carcinoma survival via the NF-kappa B/Survivin and phosphoinositide 3-kinase/Akt signaling pathways Clin Cancer Res 2010; 16:77-87. [PMID: 20028744].

41. Jen Y, Weintraub H, Benezra R. Overexpression of Id protein inhibits the muscle differentiation program: *in vivo* association of Id with E2A proteins. Genes Dev 1992; 6:1466-79. [PMID: 1644289].

42. Ke J, Wu R, Chen Y, Abba ML. Inhibitor of DNA binding proteins: implications in human cancer progression and metastasis. Am J Transl Res 2018; 10:3887-910. [PMID: 30662638].

43. Kowanetz M, Valcourt U, Bergström R, Heldin C-H, Moustakas A. Id2 and Id3 Define the potency of cell proliferation and differentiation responses to transforming growth factor β and bone morphogenetic protein. Mol Cell Biol 2004; 24:4241-54. [PMID: 15121845].

44. Wang L-H, Baker NEE. Proteins and ID Proteins: Helix-Loop-Helix Partners in development and disease. Dev Cell 2015; 35:269-80. [PMID: 26555048].

45. Chaudhary J, Sadler-Riggleman I, Ague JM, Skinner MK. The helix-loop-helix Inhibitor of Differentiation (ID) proteins induce post-mitotic terminally differentiated sertoli cells to re-enter the cell cycle and proliferate. Biol Reprod 2005; 72:1205-17. [PMID: 15647457].

Articles are provided courtesy of Emory University and the Zhongshan Ophthalmic Center, Sun Yat-sen University, P.R. China. The print version of this article was created on 25 November 2020. This reflects all typographical corrections and errata to the article through that date. Details of any changes may be found in the online version of the article.